[Imaging]

Imaging of Physeal Injury: Overuse

Shari T. Jawetz, MD,*† Parina H. Shah, MS,† and Hollis G. Potter, MD†

Context: As the intensity of youth participation in athletic activities continues to rise, the number of overuse injuries has also increased. A subset of overuse injuries involves the physis, which is extremely susceptible to injury. This paper aims to review the utility of the various imaging modalities in the diagnosis and management of physeal injuries in the skeletally immature population.

Evidence Acquisition: A search for the keywords *pediatric, physis, growth plate, x-ray, computed tomography, magnetic resonance imaging*, and *overuse injury* was performed using the PubMed database. No limits were set for the years of publication. Articles were reviewed for relevance with an emphasis on the imaging of growth plate injuries.

Study Design: Retrospective literature review.

Level of Evidence: Level 4.

Results: Three major imaging modalities (radiographs, computed tomography, and magnetic resonance imaging) complement each other in the evaluation of pediatric patients with overuse injuries. However, magnetic resonance imaging is the only modality that offers direct visualization of the physis, and it also offers the best soft tissue contrast for evaluating the other periarticular structures for concomitant injury.

Conclusion: Imaging has an important role in the diagnosis of physeal injuries, and the information it provides has a tremendous impact on the subsequent management of these patients.

Keywords: physis; overuse injuries; magnetic resonance imaging; computed tomography

Physeal injuries are common and are crucial to recognize, as morbidity and the sequelae of missed physeal injury are not easily remedied. Trauma, both acute and chronic, is by far the most common cause of physeal injury. While acute traumatic events may result in physeal damage, chronic low-grade trauma such as in overuse injuries can also injure the vulnerable growth plate. With increasing youth involvement in organized sports,[47] the phenomenon of overuse injuries is a frequent reality among children. The intense training schedules, intense focus on a single sport, and lack of off-season rest all contribute to the overuse injuries seen in children.[11,12] In the current age of competitive sports, 53% of children between the ages of 5 and 17 years sought medical care for an overuse injury in the cohort evaluated by Stracciolini et al,[58] but debate persists as to whether the incidence of pediatric sports-related injuries is actually increasing.[35] Whether the incidence of injury is trending upward, this article aims to highlight the utility of imaging in the medical workup of this patient population.

EPIDEMIOLOGY

The peak incidence of traumatic physeal injury is 11 to 12 years in girls and 13 to 14 years in boys.[20] Overall, traumatic physeal injury is relatively rare in children younger than 5 years. Physeal fractures occur twice as commonly in boys as in girls.[48]

Apart from trauma, other causes of physeal injury include infection, neoplasm, radiation, ischemia,[44] metabolic abnormalities, thermal injury, sensory neuropathy, and iatrogenic injury.[10] Epidemiologic data have shown that 18% to 30% of pediatric fractures involve the physis,[29,37,41] and 5% to 10% of physeal fractures lead to growth disturbances.[15]

PATHOANATOMY OF THE PHYSIS

Repetitive microtrauma to a tissue that supersedes the body's inherent ability to repair itself results in overuse injuries. The physis is the weakest link in the immature skeleton,[27] and the open growth plates in long bones and at apophyses render

From †Department of Radiology and Imaging, Hospital for Special Surgery, New York, New York
*Address correspondence to Shari T. Jawetz, MD, MRI Division, Hospital for Special Surgery, 535 East 70th Street, New York, NY 10021 (e-mail: jawetzs@hss.edu).
The authors report no potential conflicts of interest in the development and publication of this article.
DOI: 10.1177/1941738114559380

children more susceptible to overuse injuries.[11,12] In long bones, chronic microtrauma from overuse leads to focal or diffuse physeal widening, even in the absence of a discrete fracture line.[32] In a normal physis, osteogenesis occurs after death of chondrocytes and calcification of the chondroid matrix using the vitamin D, calcium, and phosphates supplied by the metaphyseal vessels. When the metaphyseal nutrient vessels are disrupted, the cartilage matrix does not calcify, and the persistent cartilage leads to the apparent physeal widening.[2] At apophyses, increased tension and distraction at the physis from overuse leads to chondrocyte stimulation, hypertrophy, and inflammatory changes.[1,2]

Growth disturbance, either longitudinal or angular, is the most feared complication of a physeal injury. Up to 90% of distal femoral physeal injuries lead to a growth disturbance,[3] and as distal femoral and proximal tibial growth contribute to 55% to 70% of the growth of the lower extremity, substantial limb length discrepancy may result from physeal injuries about the knee.[19] As opposed to the distal femur, the proximal femur only contributes to 30% of femoral growth; the overall risk and magnitude of limb length discrepancy resulting from physeal damage about the hip is smaller than injury about the knee.[13]

Not all physeal injuries carry the same risk of future growth disturbance. Factors affecting the likelihood of subsequent growth disturbance include degree and area of physeal injury, chronologic and skeletal age of the child, and the projected remaining growth.[15] There is a greater propensity for growth disturbance when injuries occur at the distal rather than proximal ends of the long bones.[37] Growth arrest and overuse injuries more frequently occur in the lower extremities.[3,48,58]

Subsequent to an acute growth plate injury or, less commonly, in the setting of unrelenting overuse, pathologic bridges or bars composed of osseous or fibrous tissue may develop across the physis, leading to overall reduced limb length, angular deformities, and/or altered joint biomechanics.[44] Poorly reduced fractures or fractures that extend through the osseous components of the epiphysis place patients at greatest risk of developing a physeal bar.[15] Patients who are younger at the time of initial injury are at increased risk for complications later in life.[10]

Ogden[44] described 3 main categories of physeal bridging. Type 1 bridges are peripheral and variable in size. A peripheral bridge involves the peripheral zone of Ranvier and may cause severe angular growth disturbances, which develop over short periods of time. Linear (type 2) bridges may occur anywhere within the physis, but they extend directly across the physis and may also lead to angular growth deformities. Increased transphyseal vascularity allows bony bridges to develop.[18] Type 3 (central) bridges involve the central portion of the physis; in these cases, the injured portion of the grown plate is completely surrounded by normal physis, and most commonly, these lead to longitudinal growth disturbances.

Physeal bars commonly occur at sites of physeal undulations (eg, centrally in the distal femur and peripherally in the proximal tibia).[19] The relative location of the physeal injury affects future growth disturbance; premature central physeal closure will cause limb length discrepancy without angular deformity, whereas eccentric physeal closure yields angular growth disturbances.[19]

The size of a physeal bridge affects the risk of future growth disturbance. In animal models, subsequent growth disturbance is more likely when greater than 7% of the physeal cross-sectional area is injured. Animal models have also demonstrated that bars that involve less than 7% of the cross-sectional area of the physis tend to be transient[36]; the growth of the surrounding uninjured areas of the physis causes traction and ultimately fractures the bar, allowing for resumption of normal growth.[51] Accurate characterization of the size and location of the physeal damage is important in preoperative planning.[9] Surgical resection of a physeal bar and interposition of an inert material like fat may be efficacious when the area of injury involves less than 25% of the cross-sectional area of the physis, but the best outcomes are generally achieved when less than 10% of the physeal cross-sectional area is involved. Surgical outcomes are best in younger children and are further improved when there is only a single, centrally located bar.[20]

Harris growth arrest lines, a sign of physeal damage, can be visualized on radiography, computed tomography (CT), and magnetic resonance imaging (MRI). Harris growth arrest lines occur in the setting of an inconsistent bone growth rate, and the lines generally parallel the physis. In the posttraumatic setting, absence of a Harris growth arrest line in the injured extremity may indicate complete cessation of growth. Decreasing distance between the growth arrest line and the physis suggests growth deceleration. A partial growth disturbance may manifest itself with progressive malalignment or with obliquely oriented/tethered Harris growth arrest lines.[20]

TRAUMATIC INJURIES

The most commonly used 5-type classification of traumatic physeal injuries was originally published by Salter and Harris in 1963.[53] Types 1, 2, and 5 fractures are extra-articular; intra-articular fractures (types 3 and 4) may lead to joint incongruity in addition to physeal injury.

Type 1 fractures involve only the physis. Radiographic signs include widening, haziness, sclerosis, or irregularity of the physis as well as periphyseal osteopenia. Findings may be subtle, and radiographic comparison with the contralateral, symptom-free side may be necessary.

Type 2 fractures (Figure 1) propagate along the physis and exit through a portion of the metaphysis, often yielding a triangular metaphyseal fragment (also known as a Thurston Holland fragment) because the periosteum at the physis is very tightly adherent and thus the fracture breaks through the more loosely adherent metaphyseal periosteum.[33]

Type 3 fractures (Figure 2) begin intra-articularly at the epiphyseal articular surface and extend through the epiphysis to exit through the physis.

Figure 1. Thirteen-year-old with Salter Harris type 2 fracture. (A) Coronal computed tomography (CT) image demonstrates a Thurston Holland metaphyseal fracture fragment (arrowhead). (B) Sagittal CT image demonstrates widening of the anterior aspect of the physis (arrow).

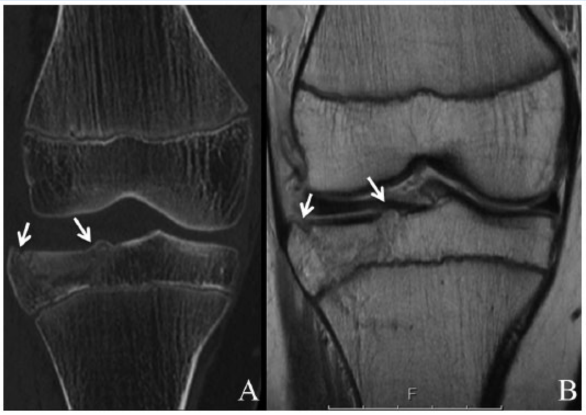

Figure 2. Seventeen-year-old male (bone age, 15 years) with Salter Harris type 3 fracture. (A) Coronal computed tomography and (B) coronal proton density magnetic resonance imaging demonstrate vertical fracture lines extending through the tibial epiphysis to the physis and there is a subtle step off of the articular surface (arrows).

Type 4 fractures also extend from the articular surface through the epiphysis and physis to exit through the metaphysis. Management of these fractures is complex, as anatomic reduction of the physis is necessary to reduce the risk of bony bar formation, and anatomic reduction of the articular surface is vital to diminish the risk of posttraumatic arthritis.

Type 5 fractures are compression or crush injuries to the physis; these fractures are the least common and the diagnosis is often missed at the time of presentation.[29]

The risk of growth disturbance is highest with types 3, 4, and 5 fractures.[45]

The injury patterns described by Salter are most often thought of in the acute trauma setting, but repetitive microtrauma often leads to type 1 physeal injuries, and even type 5 injuries are within the spectrum of overuse injuries.

PHYSEAL IMAGING

Imaging offers clinically relevant information about areas of physeal injury. In the setting of growth plate closure, it is important to be cognizant of the normal patterns of physiologic epiphysiodesis because a bar and normal physeal closure have similar imaging appearances. For example, in the distal femur, the physis begins to fuse centrally with subsequent centripetal progression of the physeal closure.[23] However, the proximal tibial physis has a different pattern of epiphysiodesis—the posterior portion fuses first with subsequent anterior progression of the closure (Figure 3).[15] In contrast, the distal tibial physis fuses initially centrally, then medially, and lateral physeal fusion occurs last.[60]

Radiography

In both the acute traumatic and chronic overuse setting, radiographs are the first-line imaging approach[10] because of accessibility and their cost-effectiveness.[54] Stress radiographs can provide insight into the degree of posttraumatic joint stability, but pain inhibition may preclude their use. Inherent to stress views is a risk that the applied stress could inadvertently injure the physis and convert a subtle Salter type 1 fracture into a displaced Salter type 3 fracture.[49]

Radiographs should be used for follow-up to assess for healing and to evaluate for malalignment and growth disturbances. The frequency of radiologic follow-up will vary based on the risk of developing posttraumatic deformities. In the setting of high-risk physeal injuries, such as distal femoral fractures, it is reasonable to obtain radiographs several times a year until a normal growth rate can be documented; the need for follow-up could range from 2 years[20] until skeletal maturity.[44] Close radiologic follow-up could identify an angular growth deformity before it is clinically apparent,[44] at which time it may be easier to correct surgically.

Noncalcified hyaline cartilage is radiolucent on radiographs, and, thus, while radiographs are important in evaluating osseous injuries, they cannot directly demonstrate injury to articular or physeal cartilage.[28] Physeal widening, epiphyseal displacement, periphyseal osteopenia, indistinctness of the epiphyseal and metaphyseal sides of the physis,[51] and fragmentation[5] are important radiographic secondary signs of acute and chronic physeal injury. In types 2 to 4 physeal fractures, the fracture lucency may be radiographically apparent within the metaphysis and/or epiphysis, but the degree of

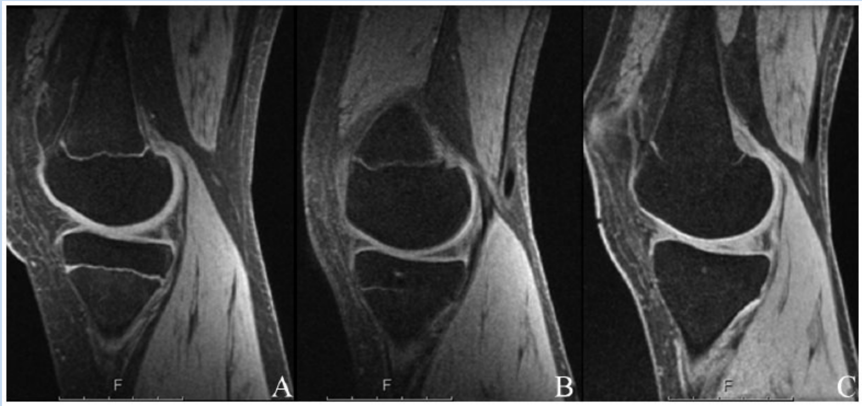

Figure 3. Sagittal 3-dimensional, fat-suppressed, T1-weighted, gradient-recalled images in the same patient at 3 time points (A, 12 years; B, 14 years, and C, 15 years) demonstrating centripetal closure of the femoral physis and physeal closure progressing from posterior to anterior in the proximal tibia.

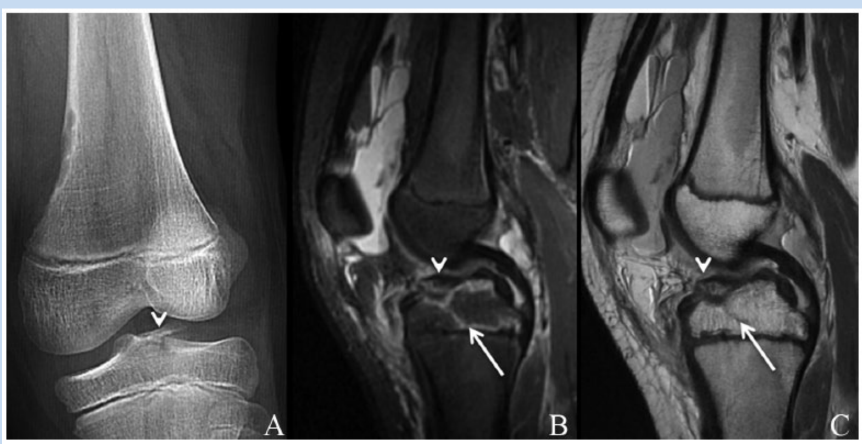

Figure 4. Ten-year-old with tibial eminence avulsion seen on (A) anterior-posterior radiograph (white arrowhead). (B) Sagittal inversion recovery and (C) fast spin echo magnetic resonance images demonstrate an additional obliquely oriented fracture line extending from the articular surface through the epiphysis to the physis (arrows), rendering this a Salter Harris 3 fracture.

involvement of the physis cannot be accurately assessed using radiographs alone.

The use of radiography in isolation has significant limitations for evaluation of pediatric periarticular fractures. Some nondisplaced fractures are radiographically occult.[51] Radiography is essentially a 2-dimensional (2D) depiction of the complex 3D physis that includes normal anatomic ridges and areas of undulation. The complex nature of the physis is difficult to evaluate when the x-ray beam is not parallel to the plane of the physis (Figure 4).[52,55] Osseous bars may be seen on radiographs, but the precise size and location of a physeal bar cannot be ascertained from radiographs alone (Figure 5). Fibrous tissue is lucent on radiographs, and a fibrous physeal bar would be missed entirely if exclusively radiographs were obtained.

Computed Tomography

Cross-sectional imaging modalities offer a more detailed analysis of the physis than radiography, and CT demonstrates further details about fracture extent and alignment, which is particularly important in evaluating the reduction of intra-articular fractures.[51] Areas of periphyseal sclerosis or osteopenia are sometimes more apparent on CT than radiographs. CT can provide accurate details about the location and extent of an osseous physeal bar, but fibrous bars and the extent of physeal damage cannot be directly evaluated as noncalcified cartilage

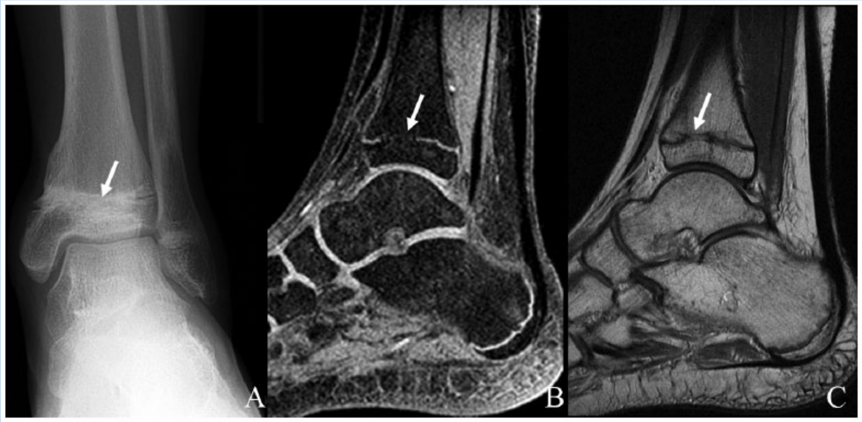

Figure 5. (A) Anterior-posterior; (B) sagittal 3-dimensional, fat-suppressed, T1-weighted, gradient-recalled; and (C) sagittal proton density images of the ankle in a 10-year-old girl with a distal tibial osseous physeal bar (white arrow) after removal of instrumentation for fracture treatment.

Table 1. Suggested computed tomography acquisition parameters for imaging the pediatric knee, utilizing both 64-slice and 16-slice scanners

Scanner	16-slice	64-slice
Scan type	Helical	Helical
Thickness, mm	0.8	0.8
Increment, mm	0.4	0.4
Voltage, kV	90 kVp	80 kVp
mAs/slice	100 mAs	50 mAs
Resolution	High	High
Pitch	0.438	0.391
Rotation time, s	0.5	0.5
Collimation	16 × 0.75	64 × 0.625

and fibrous tissue are similarly low density and thus indistinguishable on CT.

Computed tomography employs ionizing radiation for image acquisition, and the radiation doses imparted to patients are higher from CT than from radiographs.[59] When clinically indicated, CT should be utilized, but principles of radiation safety must be followed. The organs of pediatric patients are exquisitely sensitive to radiation, and a child's longer life expectancy yields a lengthier period of time during which he or she could potentially develop a radiation-induced cancer.[8] Radiation shielding should be always utilized, but especially when imaging pediatric patients. Dose should be decreased as low as reasonably achievable while maintaining diagnostic quality. Some of the newer dual-energy CT scanners offer superior bone detail with a marked reduction in dose. There are suggested parameters used for scanning a pediatric knee using both 16- and 64-slice multidetector CT scanners (Table 1).

From an economic standpoint, CT is more expensive than radiography.[42] However, the ability to postprocess isotropically acquired CT data and generate multiplanar reconstructed images and 3D reformations[50] (Figure 6) is advantageous as

Table 2. Magnetic resonance imaging acquisition parameters for imaging the pediatric knee

Parameters	3-Dimensional, Fat-Suppressed, T1-Weighted, Gradient-Recalled	Sagittal Inversion Recovery	Sagittal Proton Density	Axial Proton Density	Coronal Proton Density
Repetition time (TR), ms	12-17	4000-4500	4000-5000	5000-6000	4500-5500
Echo time (TE), ms	1.4-1.6	15-20	20-25	20-25	20-25
Slice thickness, mm	1.5	3.0-3.5	3-3.5	3-3.5	2.5-3.0
Bandwidth (BW), kHz	±20-40	±20-40	±20-40	±20-40	±20-40
Acquisition matrix	256 × 256	256 × 192	512 × 384	512 × 256	512 × 256
Field of view (FOV), cm	15-20	16-20	16-20	14-18	14-18
Number of excitations (NEX)	2	2	2	2	2

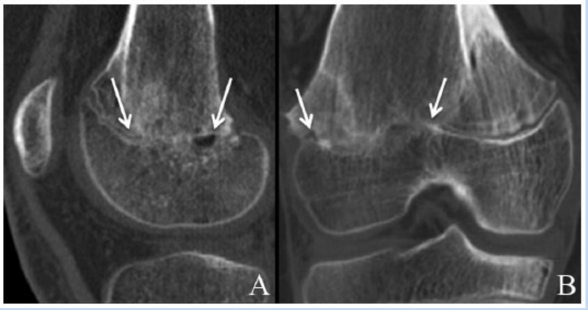

Figure 6. (A) Sagittal and (B) coronal computed tomography image of a 10-year-old boy 5 months after a distal femoral fracture with an osseous bar (arrows) across the lateral half of the distal femoral physis, resulting in varus angulation at the knee noted on concurrent radiographs.

more complex anatomic detail about an osseous physeal bar is available.

While CT is unable to directly image the physis, it remains an important imaging modality in the settings of fractures where detection and treatment of subtle incongruities is vital in helping to prevent subsequent complications (see Figure 2).

Magnetic Resonance Imaging

Jaramillo et al[28] initially described the utility of MRI in evaluating physeal injuries in an animal model. Since then, MRI sequences have been further refined, and MRI offers clinically relevant information about chronic physeal injury, osseous and fibrous physeal bridges, epiphyseal and metaphyseal avascular necrosis, and growth arrest.[51] MRI can demonstrate the location, morphology,[21] and precise size of a physeal injury.[30] In the small population of patients in whom MRI is contraindicated, CT (with or without arthrography) provides information that cannot be obtained through radiography alone.

Magnetic resonance imaging offers high spatial resolution, superior soft tissue contrast, and direct and indirect multiplanar imaging capabilities without ionizing radiation.[49] Compared with radiography and CT, MRI is more expensive, and the acquisition and postprocessing is more time intensive, but it is recommended because it provides a noninvasive means of directly visualizing physeal and articular cartilage.[52]

Magnetic resonance imaging should be performed on a clinical 1.5-tesla (T) or 3.0-T magnet using a surface coil (Table 2).

The 3D, frequency-selected, fat-suppressed, T1-weighted, gradient-recalled images are the most useful in evaluating physeal hyaline cartilage.[14] The 3D nature of the sequence allows users to reformat the images into additional planes after image acquisition; thus, it is only necessary to acquire the 3D, fat-suppressed, T1-weighted, gradient-recalled images in a single plane, thereby diminishing the time of image acquisition. While it is not necessary to do so, it may be helpful to acquire the 3D, fat-suppressed, T1-weighted, gradient-recalled data in a plane orthogonal to the physis so that a qualitative assessment of physeal integrity can be made without further post-processing. Isotropic voxel acquisition promotes superior reconstruction; however, maximizing through plane (slice thickness) resolution is the best means by which to impart more accurate assessment of the physeal bar volume. For example, an adolescent knee should use slice thickness of no more than 1.5 mm with no interslice gap.

On fat-suppressed, T1-weighted, gradient echo images, hyaline cartilage is high signal whereas the fatty marrow signal is

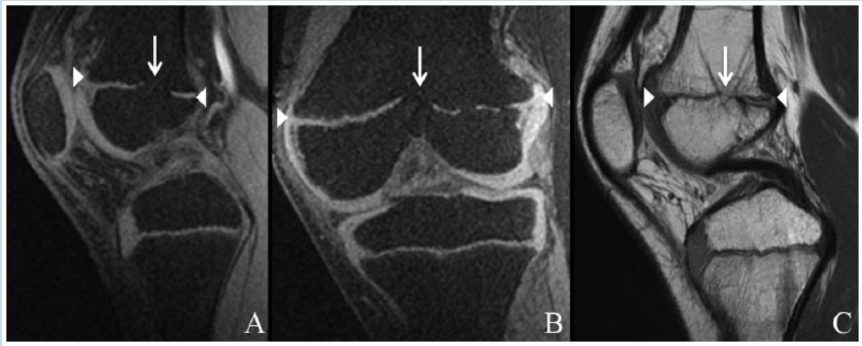

Figure 7. Thirteen months after a distal femoral fracture with an osseous bar located centrally within the distal femoral physis. (A) Sagittal and (B) coronal 3-dimensional, fat-suppressed, T1-weighted, gradient-recalled magnetic resonance images demonstrate the bridge (white arrows) as abnormal low signal intensity crossing the central physis (white arrowheads). At the peripheral margins, the physeal cartilage is indistinguishable from the articular cartilage (white arrowheads). (C) Sagittal proton density image demonstrates that signal within the bar (white arrow) is isointense to the adjacent bone, indicating its osseous composition.

suppressed by spectrally selective preparatory pulses, and the mineralized bony trabeculae render the osseous structures low signal.[26] This striking difference in signal intensity yields the excellent contrast resolution between the cartilage and the adjacent epiphyseal and metaphyseal bone. A normal growth plate appears as a uniform high signal intensity line extending across the width of the bone. A focus of physeal disruption will appear as a defined area of abnormal low signal intensity within the high-signal-intensity physis.[19] However, as all hyaline cartilage appears as high signal on the 3D, fat-suppressed, T1-weighted, gradient-recalled sequences, there is no distinction between the high signal intensity physeal and articular cartilage (Figure 7). As a result, the edges of the physis may be difficult to distinguish from the articular surface.[10,52] Evaluating the physis in multiple planes can help overcome this limitation, and this interface may require some manual correction when using semi-automated 3D modeling algorithms.

In cases of physeal damage, MRI demonstrates subtle physeal widening and irregularity. Fluid-sensitive inversion recovery or frequency-selective fat-saturated T2 sequences may demonstrate edema (high signal) along the physis, which indicates injury (see Figure 4).[27] In acute to subacute Salter-Harris fractures that extend into the epiphysis and/or metaphysis, the bone marrow edema pattern will be present about the physis and within the involved segment of the bone. Because of its tomographic nature and superior soft tissue contrast, often a fracture line is more apparent on MRI than other imaging modalities (Figures 4 and 8).

Apart from a focal defect in the physis, metaphyseal intrusions of physeal cartilage are another sign of physeal damage, where the physeal cartilage extends beyond the growth plate into the metaphysis.[34] Chronic metaphyseal intrusions that become fixed within the metaphyseal bone lead to discrete islands of physeal cartilage within the metaphysis (Figure 9).[10] No known association exists between the presence of metaphyseal intrusions and the cause of physeal injury.[19]

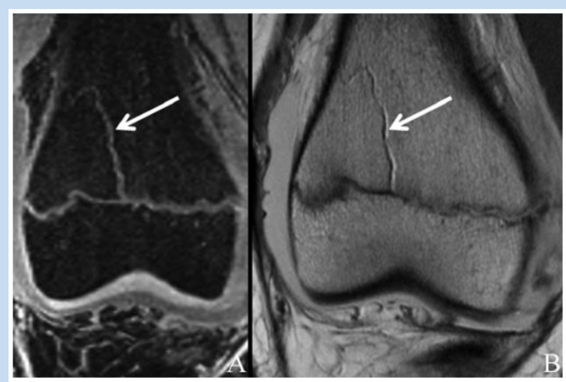

Figure 8. Fifteen-year-old injured playing soccer. Magnetic resonance image was obtained to exclude cruciate and collateral ligament injury. (A) Coronal 3-dimensional, fat-suppressed, T1-weighted, gradient-recalled and (B) proton density images demonstrate a Salter Harris type 2 fracture (white arrows).

Metal susceptibility results in artifact on gradient echo images, and this could limit the use of the 3D, fat-suppressed, T1-weighted, gradient-recalled sequence postoperatively. Depending on their composition, different metals yield varying degrees of susceptibility. At the time of surgery, imperceptible tiny foci of metallic debris are shed from surgical instruments such that susceptibility artifact may obscure the physis even without metallic fixation. The history of prior surgery, however, is not a contraindication for use of the 3D, fat-suppressed, T1-weighted, gradient-recalled sequence. In fact, at our

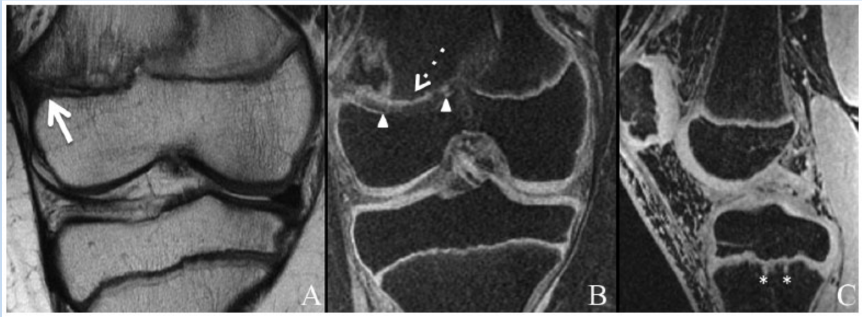

Figure 9. Coronal (A) proton density and (B) 3-dimensional (3D), fat-suppressed, T1-weighted, gradient-recalled images from the patient shown in Figure 6 demonstrate physeal irregularity (solid white arrow) and a metaphyseal island of physeal cartilage (hatched arrow) in an area where the physis is closed (arrowheads). (C) Sagittal 3D, fat-suppressed, T1-weighted, gradient-recalled image from an 11-year-old boy demonstrates intrusions of physeal cartilage into the proximal tibial metaphysis (asterisks).

Figure 10. (A and B) Sagittal 3-dimensional, fat-suppressed, T1-weighted, gradient-recalled magnetic resonance images from a 13-year-old 3 months after all epiphyseal anterior cruciate ligament reconstruction demonstrate no injury to the distal femoral physis adjacent to the epiphyseal fixation (arrowhead). Arrow in image B demonstrates a small area of physeal disturbance anteriorly in the proximal tibia.

institution, MRI is often obtained after anterior cruciate or medial patellofemoral ligament reconstruction in skeletally immature patients to evaluate for postoperative physeal damage (Figure 10).

Physeal bridges have been identified at imaging as early as 2 months after injury, but the mean time to detection of a bar is 1 year (median, 10.8 months).[19] When present, MRI can help characterize the composition of a physeal bar. On proton density fast spin echo images, osseous tissue is high in signal intensity because of the presence of fatty marrow, whereas fibrous tissue is low in signal intensity (Figure 7). Osseous bridges involving <25% of the cross-sectional area of the physis are of variable signal intensity, but large bony bars are isointense or slightly hyperintense to the metaphyseal marrow on T1-weighted images.[19] Low signal intensity adjacent to the physis on proton density images indicates periphyseal sclerosis (Figure 11) and underlying physeal injury. Harris growth arrest lines are also apparent on proton density images but not on the 3D, fat-suppressed, T1-weighted, gradient-recalled images.

In the setting of both acute and overuse injuries, an MRI can provide insight into the extent and pattern of physeal injury and can demonstrate non–growth plate–related injuries about the joint of interest. An MRI examination obtained in the acute setting may also serve as a baseline to which future studies can be compared.

The 3D, fat-suppressed, T1-weighted, gradient-recalled datasets can be analyzed qualitatively and quantitatively. Simply by scrolling through the stacked 3D, fat-suppressed, T1-weighted, gradient-recalled images, the presence and relative location of a focal physeal closure can be appreciated. Through visual analysis of the size of the defect, one can estimate a rough percentage of involvement. Many picture archiving and communications systems include software that allows users to create a physeal map using maximum intensity projection images generated from the MRI data.[19] Using commercially available software, users can manually segment the physis and calculate the physeal surface area.[4,9] Koff et al[30] and Lurie et al[34] described the use of semi-automated physeal segmentation using customized software. After physeal segmentation, postprocessing tools allow for calculation of the absolute and relative area of physeal damage and/or bar. Of note, validation of software is a requisite for accurate, reproducible assessment of the magnitude of physeal interruption, typically with a preclinical model of focal physeal ablation.[30] Once the physis is segmented, 3D models can be created to demonstrate the shape, size, and location of the physeal damage (Figure 12).[34] These quantitative data are clinically relevant in the prediction

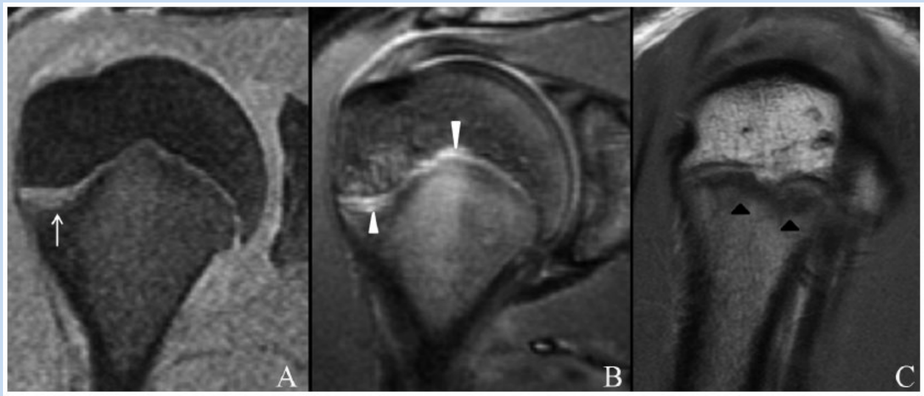

Figure 11. Thirteen-year-old pitcher. Oblique coronal (A) 3-dimensional, fat-suppressed, T1-weighted, gradient-recalled and (B) inversion recovery as well as (C) oblique sagittal proton density magnetic resonance images demonstrating physeal widening (arrow) and minimal edema (white arrowheads) as well as sclerosis on the metaphyseal side (black arrowheads) indicating chronicity.

of potential limb length discrepancy and for purposes of operative planning.

The nonphyseal structures are best evaluated on high-resolution fast spin echo images.[49] At our institution, all pediatric joints are imaged with a protocol that includes a single plane acquisition of the 3D, fat-suppressed, T1-weighted, gradient-recalled image, a single plane of inversion recovery sequence, as well as 3 planes (sagittal, axial, and coronal) of proton density. The proton density and inversion recovery images nicely demonstrate pathology of the articular cartilage and periarticular ligamentous, muscular, and tendinous structures, as well as periarticular neural and vascular structures.

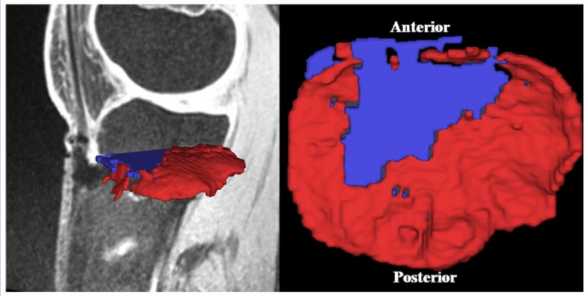

Figure 12. Sagittal 3-dimensional (3D), fat-suppressed, T1-weighted, gradient-recalled image with superimposed 3D model of the physeal bar where the red indicates the normal physis and the blue represents the bar. The 3D model has been virtually "extracted" from the planar image. The physis and bar area were calculated from the 3D model. Physis area, 2553.7 mm^2; bar area, 698.6 mm^2; percentage bar, 27.4%.

OVERUSE INJURIES

Upper Extremity

Overuse injury in the wrist, commonly referred to as "gymnast wrist," is essentially a type 1 physeal fracture due to repetitive weightbearing and direct impaction on the wrist.[56] When the repetitive microtrauma continues without opportunity to heal, a distal radius physeal bridge may form, resulting in premature growth arrest. As the ulna continues to grow normally, the relative overgrowth of the ulna (positive ulnar variance)[6] may lead to injury of the triangular fibrocartilage complex and ulnolunate impaction (Figure 13).[33]

In the elbow, "little leaguer's elbow" is a nonspecific term that often refers to medial epicondylar physeal overuse injury secondary to chronic traction from excessive valgus forces that occur during the pitching motion. Initial radiographs are negative in 85% of cases.[25] Medial epicondylar apophysitis most commonly occurs between the ages of 9 and 12.[24] When longstanding and severe, there may be partial or complete avulsion of the apophysis (Figure 14). With chronic traction, the medial epicondylar apophysis may have an enlarged, bulbous appearance because of overgrowth secondary to chronic stress.[17,25] Once the medial epicondylar physis has fused (typically by age 17 in boys and 14 in girls),[46] patients are more likely to injure the medial (ulnar) collateral ligament (MCL). As opposed to adults, in children, injury to the medial collateral ligament tends to be an acute injury rather than a chronic overuse injury.[22]

Traumatic and overuse injuries can also occur about the olecranon apophysis. In the setting of chronic overuse, there can be a stress fracture through or delayed closure of the olecranon physis,[39] which typically fuses at age 14 years in girls and at age 16 years in boys.[46] Radiographically, this injury can

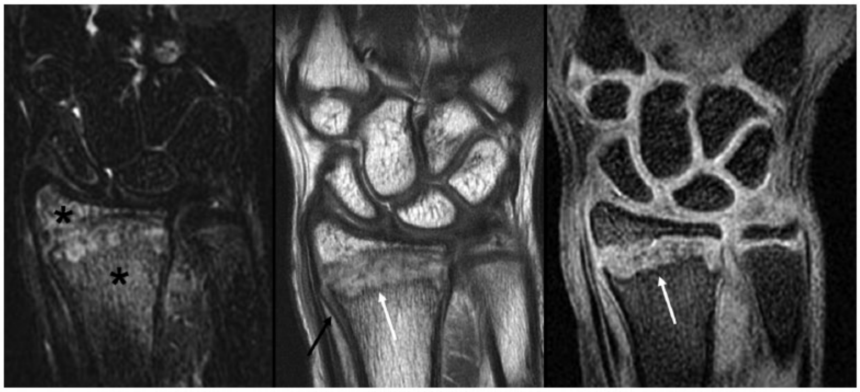

Figure 13. Nine-year-old gymnast with chronic mechanical stress leading to physeal injury of distal radius where there is bone marrow edema (asterisk), periosteal new bone formation (black arrow), and physeal widening (white arrows) secondary to chronic stress.

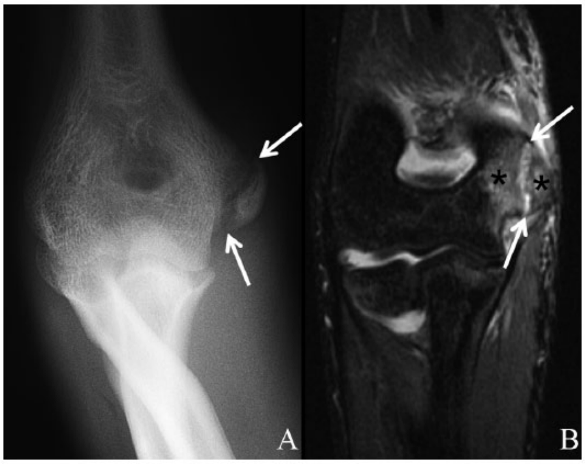

Figure 14. Fifteen-year-old pitcher with acute onset pain while playing baseball. (A) Oblique radiograph and (B) coronal inversion recovery magnetic resonance image demonstrate widening of the medial epicondylar physis (arrow) with adjacent apophyseal edema (asterisk).

be difficult to appreciate, and contralateral radiographs may be indicated (Figure 15).[17,25,39]

Proximal humeral physeal injury (commonly referred to as "little leaguer's shoulder") was first described in 1953 by Dotter[16] and commonly occurs in children ages 11 to 16 years, during a time of peak growth.[5,38,40] Injury occurs because of repetitive traction and rotational torque stresses from throwing and other overhead activities.[24] Imaging findings are similar to those of other stress-related physeal injuries (Figure 11).[43]

Pelvis and Lower Extremity

Injuries at any of the numerous apophyses, including the iliac crests (abdominal muscles), anterior superior (sartorius) and inferior iliac spines (rectus femoris), greater (abductors) and lesser (iliopsoas) trochanters, and ischial tuberosities (hamstrings) may occur in the setting of acute trauma or chronic overuse (Figure 16).[31] In the setting of chronic injury, the abundant callus formation seen on radiographs about the apophysis may appear neoplastic; in these confusing cases, it is best to obtain imaging follow-up or cross-sectional imaging to demonstrate the healing fracture so that more unwarranted aggressive action is avoided.[7] Of note, whereas in adults lesser trochanter avulsion injuries occur most commonly in the setting of malignancy, they are typically benign in children.[7]

Typically seen in the setting of repetitive jumping, squatting, and kneeling, Osgood Schlatter disease is a chronic traction apophysitis at the tibial tubercle and Sinding Larsen Johannson is traction apophysitis at the inferior pole of the patella (Figure 17).[57] In addition to the typical radiographic findings of physeal injury, these patients may also have a thickened patellar tendon. MRI can demonstrate partial tears of the tendon that might alter patient management.[7]

Calcaneal apophysitis, also known as Sever disease, is more common in boys who participate in running sports. It may be because of growth spurts, but traction from the gastrocnemius-soleus complex can lead to apophysitis at the calcaneal apophysis. While calcaneal apophysitis is often a clinical diagnosis, imaging may be obtained to exclude other causes of heel pain such as a calcaneal stress fracture.[7]

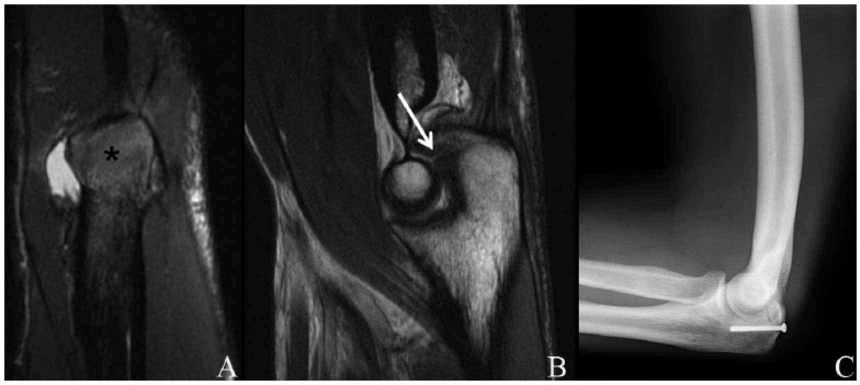

Figure 15. Sixteen-year-old pitcher with delayed olecranon apophyseal union. (A) Coronal inversion recovery and (B) sagittal proton density images demonstrate a stress reaction with bone marrow edema (asterisk) about an unfused olecranon apophysis (arrow). (C) Patient underwent pin fixation as seen on the lateral radiograph.

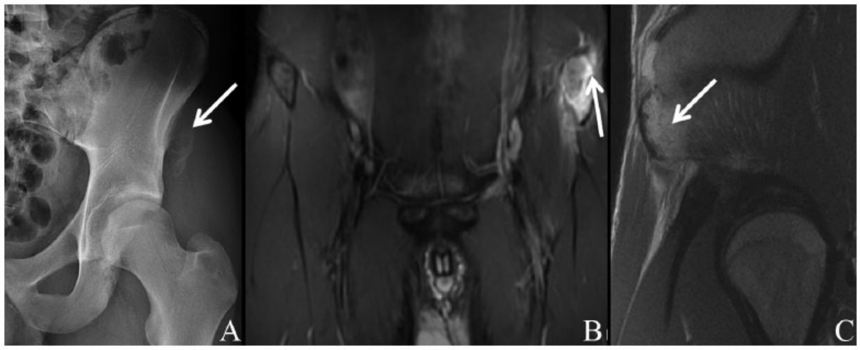

Figure 16. Seventeen-year-old male track and field athlete with (A) anterior-posterior radiograph, (B) coronal inversion recovery, and (C) sagittal proton density images demonstrating an acute avulsion of the anterosuperior iliac spine (arrow).

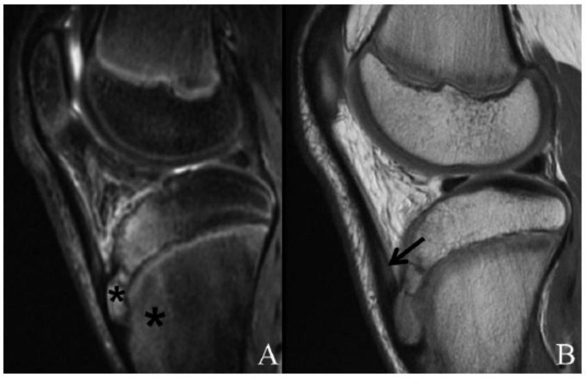

Figure 17. Twelve-year-old soccer, basketball, and lacrosse player with anterior knee pain. (A) Sagittal inversion recovery and (B) proton density images demonstrate bone marrow edema about the tibial tubercle apophysis (asterisks) and within the metaphysis, indicative of Osgood Schlatter disease. Thickening and high signal intensity of the patellar tendon (black arrow) indicates patellar tendinosis.

CONCLUSION

Noninvasive imaging is extremely important in the management of pediatric patients with physeal injuries, both in the acute traumatic and chronic overuse settings. Radiographs and CT have roles in evaluating these injuries, but one must remain cognizant of patient exposure to ionizing radiation. MRI offers clinically relevant information without ionizing radiation. Knowledge of the location and extent of physeal damage and injury to the extraphyseal structures allows for a more comprehensive assessment of the risk of future complications. Information obtained from imaging studies has an important role in patient counseling and management as well as preoperative planning. Clinical information achieved through imaging may lead to significant alterations in patient management.

REFERENCES

1. Alberty A, Peltonen J. Proliferation of the hypertrophic chondrocytes of the growth plate after physeal distraction. An experimental study in rabbits. *Clin Orthop Relat Res*. 1993;(297):7-11.

2. Apte SS, Kenwright J. Physeal distraction and cell proliferation in the growth plate. *J Bone Joint Surg Br*. 1994;76:837-843.
3. Basener CJ, Mehlman CT, DiPasquale TG. Growth disturbance after distal femoral growth plate fractures in children: a meta-analysis. *J Orthop Trauma*. 2009;23:663-667.
4. Borsa JJ, Peterson HA, Ehman RL. MR imaging of physeal bars. *Radiology*. 1996;199:683-687.
5. Carson WG Jr, Gasser SI. Little Leaguer's shoulder. A report of 23 cases. *Am J Sports Med*. 1998;26:575-580.
6. Chang CY, Shih C, Penn IW, Tiu CM, Chang T, Wu JJ. Wrist injuries in adolescent gymnasts of a Chinese opera school: radiographic survey. *Radiology*. 1995;195:861-864.
7. Chang GH, Paz DA, Dwek JR, Chung CB. Lower extremity overuse injuries in pediatric athletes: clinical presentation, imaging findings, and treatment. *Clin Imaging*. 2013;37:836-846.
8. Costello JE, Cecava ND, Tucker JE, Bau JL. CT radiation dose: current controversies and dose reduction strategies. *AJR Am J Roentgenol*. 2013;201:1283-1290.
9. Craig JG, Cody DD, Van Holsbeeck M. The distal femoral and proximal tibial growth plates: MR imaging, three-dimensional modeling and estimation of area and volume. *Skeletal Radiol*. 2004;33:337-344.
10. Craig JG, Cramer KE, Cody DD, et al. Premature partial closure and other deformities of the growth plate: MR imaging and three-dimensional modeling. *Radiology*. 1999;210:835-843.
11. Davis KW. Imaging pediatric sports injuries: lower extremity. *Radiol Clin North Am*. 2010;48:1213-1235.
12. Davis KW. Imaging pediatric sports injuries: upper extremity. *Radiol Clin North Am*. 2010;48:1199-1211.
13. Dimeglio A. Growth in pediatric orthopaedics. *J Pediatr Orthop*. 2001;21:549-555.
14. Disler DG. Fat-suppressed three-dimensional spoiled gradient-recalled MR imaging: assessment of articular and physeal hyaline cartilage. *AJR Am J Roentgenol*. 1997;169:1117-1123.
15. Dodwell ER, Kelley SP. Physeal fractures: basic science, assessment and acute management. *Orthop Trauma*. 2011;25:377-391.
16. Dotter WE. Little Leaguer's shoulder: a fracture of the proximal epiphysial cartilage of the humerus due to baseball pitching. *Guthrie Clin Bull*. 1953;23:68-72.
17. Dwek JR, Chung CB. A systematic method for evaluation of pediatric sports injuries of the elbow. *Pediatr Radiol*. 2013;43(suppl 1):S120-S128.
18. Ecklund K, Jaramillo D. Imaging of growth disturbance in children. *Radiol Clin North Am*. 2001;39:823-841.
19. Ecklund K, Jaramillo D. Patterns of premature physeal arrest: MR imaging of 111 children. *AJR Am J Roentgenol*. 2002;178:967-972.
20. Escott BG, Kelley SP. Management of traumatic physeal growth arrest. *Orthop Trauma*. 2012;26:200-211.
21. Futami T, Foster BK, Morris LL, LeQuesne GW. Magnetic resonance imaging of growth plate injuries: the efficacy and indications for surgical procedures. *Arch Orthop Trauma Surg*. 2000;120:390-396.
22. Greiwe RM, Saifi C, Ahmad CS. Pediatric sports elbow injuries. *Clin Sports Med*. 2010;29:677-703.
23. Harkes G, Dankert J, Feijen J. Growth of uropathogenic *Escherichia coli* strains at solid surfaces. *J Biomater Sci Polym Ed*. 1992;3:403-418.
24. Hoang QB, Mortazavi M. Pediatric overuse injuries in sports. *Adv Pediatr*. 2012;59:359-383.
25. Iyer RS, Thapa MM, Khanna PC, Chew FS. Pediatric bone imaging: imaging elbow trauma in children—a review of acute and chronic injuries. *AJR Am J Roentgenol*. 2012;198:1053-1068.
26. Jaimes C, Chauvin NA, Delgado J, Jaramillo D. MR imaging of normal epiphyseal development and common epiphyseal disorders. *Radiographics*. 2014;34:449-471.
27. Jaimes C, Jimenez M, Shabshin N, Laor T, Jaramillo D. Taking the stress out of evaluating stress injuries in children. *Radiographics*. 2012;32:537-555.
28. Jaramillo D, Shapiro F, Hoffer FA, et al. Posttraumatic growth-plate abnormalities: MR imaging of bony-bridge formation in rabbits. *Radiology*. 1990;175:767-773.
29. Kawamoto K, Kim WC, Tsuchida Y, et al. Incidence of physeal injuries in Japanese children. *J Pediatr Orthop B*. 2006;15:126-130.
30. Koff MF, Chong le R, Virtue P, et al. Correlation of magnetic resonance imaging and histologic examination of physeal bars in a rabbit model. *J Pediatr Orthop*. 2010;30:928-935.
31. Kovacevic D, Mariscalco M, Goodwin RC. Injuries about the hip in the adolescent athlete. *Sports Med Arthrosc*. 2011;19:64-74.
32. Laor T, Wall EJ, Vu LP. Physeal widening in the knee due to stress injury in child athletes. *AJR Am J Roentgenol*. 2006;186:1260-1264.
33. Little JT, Klionsky NB, Chaturvedi A, Soral A, Chaturvedi A. Pediatric distal forearm and wrist injury: an imaging review. *Radiographics*. 2014;34:472-490.
34. Lurie B, Koff MF, Shah P, et al. Three-dimensional magnetic resonance imaging of physeal injury: reliability and clinical utility. *J Pediatr Orthop*. 2014;34:239-245.
35. Lykissas MG, Eismann EA, Parikh SN. Trends in pediatric sports-related and recreation-related injuries in the United States in the last decade. *J Pediatr Orthop*. 2013;33:803-810.
36. Mäkelä EA, Vainionpää S, Vihtonen K, Mero M, Rokkanen P. The effect of trauma to the lower femoral epiphyseal plate. An experimental study in rabbits. *J Bone Joint Surg Br*. 1988;70:187-191.
37. Mann DC, Rajmaira S. Distribution of physeal and nonphyseal fractures in 2,650 long-bone fractures in children aged 0-16 years. *J Pediatr Orthop*. 1990;10:713-716.
38. Mariscalco MW, Saluan P. Upper extremity injuries in the adolescent athlete. *Sports Med Arthrosc*. 2011;19:17-26.
39. Matsuura T, Kashiwaguchi S, Iwase T, Enishi T, Yasui N. The value of using radiographic criteria for the treatment of persistent symptomatic olecranon physis in adolescent throwing athletes. *Am J Sports Med*. 2010;38:141-145.
40. May MM, Bishop JY. Shoulder injuries in young athletes. *Pediatr Radiol*. 2013;43(suppl 1):S135-S140.
41. Mizuta T, Benson WM, Foster BK, Paterson DC, Morris LL. Statistical analysis of the incidence of physeal injuries. *J Pediatr Orthop*. 1987;7:518-523.
42. Murray K, Nixon GW. Epiphyseal growth plate: evaluation with modified coronal CT. *Radiology*. 1988;166:263-265.
43. Obembe OO, Gaskin CM, Taffoni MJ, Anderson MW. Little Leaguer's shoulder (proximal humeral epiphysiolysis): MRI findings in four boys. *Pediatr Radiol*. 2007;37:885-889.
44. Ogden JA. The evaluation and treatment of partial physeal arrest. *J Bone Joint Surg Am*. 1987;69:1297-1302.
45. Ogden JA. Injury to the growth mechanisms of the immature skeleton. *Skeletal Radiol*. 1981;6:237-253.
46. Pappas AM. Elbow problems associated with baseball during childhood and adolescence. *Clin Orthop Relat Res*. 1982;(164):30-41.
47. Paterno MV, Taylor-Haas JA, Myer GD, Hewett TE. Prevention of overuse sports injuries in the young athlete. *Orthop Clin North Am*. 2013;44:553-564.
48. Peterson HA, Madhok R, Benson JT, Ilstrup DM, Melton LJ 3rd. Physeal fractures: part 1. Epidemiology in Olmsted County, Minnesota, 1979-1988. *J Pediatr Orthop*. 1994;14:423-430.
49. Potter HG. Imaging of the multiple-ligament-injured knee. *Clin Sports Med*. 2000;19:425-441.
50. Rogalla P, Kloeters C, Hein PA. CT technology overview: 64-slice and beyond. *Radiol Clin North Am*. 2009;47:1-11.
51. Rogers LF, Poznanski AK. Imaging of epiphyseal injuries. *Radiology*. 1994;191:297-308.
52. Sailhan F, Chotel F, Guibal AL, et al. Three-dimensional MR imaging in the assessment of physeal growth arrest. *Eur Radiol*. 2004;14:1600-1608.
53. Salter RB, Harris WR. Injuries involving the epiphyseal plate. *J Bone Joint Surg*. 1963;45:587-622.
54. Sanchez TR, Jadhav SP, Swischuk LE. MR imaging of pediatric trauma. *Magn Reson Imaging Clin North Am*. 2009;17:439-450.
55. Shi DP, Zhu SC, Li Y, Zheng J. Epiphyseal and physeal injury: comparison of conventional radiography and magnetic resonance imaging. *Clin Imaging*. 2009;33:379-383.
56. Shih C, Chang CY, Penn IW, Tiu CM, Chang T, Wu JJ. Chronically stressed wrists in adolescent gymnasts: MR imaging appearance. *Radiology*. 1995;195:855-859.
57. Stevens MA, El-Khoury GY, Kathol MH, Brandser EA, Chow S. Imaging features of avulsion injuries. *Radiographics*. 1999;19:655-672.
58. Stracciolini A, Casciano R, Levey Friedman H, Stein CJ, Meehan WP 3rd, Micheli LJ. Pediatric sports injuries: a comparison of males versus females. *Am J Sports Med*. 2014;42:965-972.
59. Vallier HA, Ahmadinia K, Forde FA, Ekstein C, Nash CL Jr, Tornetta P 3rd. Trends in musculoskeletal imaging for trauma patients: how has our practice changed over time? *J Orthop Trauma*. 2014;28:e236-e241.
60. White JR, Wilsman NJ, Leiferman EM, Noonan KJ. Histomorphometric analysis of an adolescent distal tibial physis prior to growth plate closure. *J Child Orthop*. 2008;2:315-319.